

STOCHASTIC RESONANCE DUE TO THERMALLY INDUCED NOISE IN A BISTABLE POTENTIAL

A thesis submitted to the School of Graduate Studies
Addis Ababa University



In partial Fulfilment of the Requirements for the
Degree of Master of Science in Physics

By

Bekele Jemama

Addis Ababa, Ethiopia

July 2007

ADDIS ABABA UNIVERSITY
FACULTY OF SCIENCE
DEPARTMENT OF PHYSICS

The undersigned hereby certify that they have read and recommended to the Faculty of Science School of Graduate Studies for acceptance a thesis entitled “**Stochastic Resonance due to Thermally induced noise in a bistable potential**” by **Bekele Jemama** in partial fulfillment of the requirements for the degree of **Master of Science in Physics**.

Name

Signature

Dr. Mulugeta Bekele, Advisor

Prof. Singh P., Examiner

Dr. Tewari H. S., Examiner

To my entire parents.

Acknowledgements

First and foremost, I would like to thank the almighty, *God*. I would also like to thank my advisor and supervisor Dr. Mulugeta Bekele for his unreserved support, excellent and generous guidance throughout my work. While working with him, I have got not only a chance to share his long research experience which benefited me a lot but also how to build up social life and friendly relationship with people. I am also indebted to Mr. Fikadu Legesse for his invaluable comments on every contents of the thesis. He has been guiding, assisting, editing, making numerous corrections and improvements in this work. I am extremely grateful to my *lovely* friend Miss. Rahel Dubiwak for her persistent support and invaluable advice. Of course, I am grateful to my parents for their support, patience and *love*. Without them, this work would never have come to existence(literally). Finally, a special thought also goes to Haramaya University for its continuous financial support during my study leave without which the successful completion of this thesis would have ended a day dream.

Addis Ababa, Ethiopia

Bekele Jemama

Abstract

Stochastic resonance is an essentially nonlinear phenomenon, requiring the presence of an energetic activation barrier, a weak coherent input signal and a source of noise whereby generally feeble input information such as a weak signal can be amplified and optimized by the assistance of noise. In order to study this phenomenon, we propose a model which enable us to convert a monostable potential to a bistable one through a mechanism called belowtorch effect. Having successfully established the bistable potential, we consider motion of a Brownian particle subjected to random force describing noise and weak periodic force in a highly viscous non-homogenous medium and the bistable potential with spatially varying background temperature. We use a numerical technique to compute some of the observables (such as signal-to-noise-ratio and spectral amplification) that are actually used to quantify stochastic resonance. The result shows that the response of the system undergoes resonance-like behavior as a function of hot temperature. The existence of this resonance-like behavior is still the identifying characteristic of the stochastic resonance phenomenon.

Table of Contents

Table of Contents	vi
List of Figures	viii
1 Introduction	1
2 General Features of Stochastic Resonance in a Bistable Potential	7
2.1 Characterization of stochastic resonance	8
2.2 System response to the periodic forcing	13
2.3 The autocorrelation function	18
2.4 The power spectral density	18
2.5 Spectral power amplification	20
2.6 Signal-to-noise-ratio(SNR)	22
3 Stochastic resonance due to thermally induced noise in bistable system	24
3.1 Impurity diffusion in a non-homogeneous temperature	25
3.2 Mean first passage time and escape rate	31
3.2.1 The high barrier limit approach	33
3.2.2 The exact numerical technique	34
4 Result and discussion	35
4.1 Amplitude of the periodic response	37
4.2 Spectral amplification	39
4.3 Signal output power	40
4.4 Noise output power	41
4.5 Signal-To-Noise-Ratio	42
5 Summary And conclusion	45

Appendix	48
Bibliography	50

List of Figures

1.1	Brief illustration of the stochastic resonance mechanism	4
2.1	Typical behavior of the system response characteristic versus noise strength with $\Omega = 0.005Hz$, $\Delta V = 0.25eV$, $A_0 = 0.1$, and $x_m = 1$. . .	15
2.2	Single realization of $x(t)$ in the periodically modulated double-well potential, Eq. (2.5), with modulation amplitude $A_0 = 0.1$, modulation frequency $\Omega = 0.005Hz$, $\Delta t = 0.05sec$ and $\Delta V = 0.25eV$ for three different values of noise strength D	17
2.3	Plot of spectral power amplification versus noise strength with $\Omega = 0.005Hz$, $\Delta V = 0.25eV$, $A_0 = 0.1$, and $x_m = 1$	22
2.4	SNR as a function of noise strength with $\Omega = 0.005Hz$, $\Delta V = 0.25eV$, $A_0 = 0.1$, and $x_m = 1$	23
3.1	Plots of effective potentials as a function of position for $T_H = 35K$, $65K$, $95K$, $125K$ from bottom to top with $T_C = 300K$, $\mu = 5.43nm$, $V_0 = 0.125eV$, $\Phi = 10V_0$, $n = 0.5$ (left), $n = 1.0$ (right).	29
4.1	Exact and Approximate values of mean first passage time as a function of hot temperature for $n = 0.5$ (left) and $n = 1.0$ (right).	36
4.2	Exact and Approximate values of Transition rate versus hot temperature for $n = 0.5$ (left) and $n = 1.0$ (right).	36

4.3	Amplitude of a periodic component of the system response versus hot temperature at a fixed periodic frequency, Ω , for different values of periodic amplitude with $n = 0.5$ (left) and $n = 1.0$ (right).	38
4.4	Amplitude of a periodic component of the system response as a function of hot temperature at a fixed modulation amplitude of $A_0 = 0.1$ for different values of deriving frequency with $n = 0.5$ (left) and $n = 1.0$ (right).	38
4.5	Spectral Amplification as a function of hot temperature for different values of the periodic frequency and $n = 0.5$ (left) and $n = 1.0$ (right).	40
4.6	Signal output power as a function of hot temperature for $n = 0.5$ (left) and $n = 1.0$ (right) with different values of periodic amplitude.	41
4.7	Noise output power versus hot temperature for fixed value of periodic amplitude and $n = 0.5$ (left) and $n = 1.0$ (right).	42
4.8	SNR as a function of hot temperature for $n = 0.50$ (left) and $n = 1.0$ (right) with different modulation amplitude.	43
4.9	SNR for the case of $n = 1.0$ as a function of Hot temperature for different values of Ω and $A_0 = 0.1$ with $n = 0.5$.(left) and $n = 1.0$ (right)	43
4.10	SNR (left) and spectral amplification (right) as a function of Hot temperature for different values of the parameter n with $A_0 = 0.1$ and $\Omega = 68\mu Hz$	44

Chapter 1

Introduction

Two sweeping generalizations can be made about most natural systems. They are intrinsically nonlinear and operate in noisy environments [1]. In everyday life, noise is generally viewed as being of harmful influence in detecting and transferring information. However, during the last two decades, the paradigm of stochastic resonance proved these assertions wrong: indeed, addition of the appropriate amount of noise can boost a signal and hence facilitate its detection in a noisy environment. Stochastic resonance refers to a situation where the mere addition of random noise to the dynamics improves a system's sensitivity to discriminate weak information carrying signals [1, 2]. Thus, this phenomenon constitutes yet another example where random perturbations play a useful role in enhancing detection and aiding the transmission efficiency of weak information in nonlinear systems.

The term stochastic resonance was originally coined in 1981 by Roberto Benzi and his coworkers in the context of modelling the switching of the earth's climate between ice ages and periods of relative warmth with a period of about 100,000 years [2, 3]. The eccentricity of the earth's orbit varies with that period, but the variation is not strong enough to cause such dramatic climatic changes. In the proposed model the

global climate is characterized by the position of a particle moving in double-well potential. The corresponding potential minima represent ice ages with low temperatures and normal, relatively warmth, climate cycles respectively. The potential is subjected to small periodic forcing which reflects the modulation of the eccentricity of earth's orbit. Usual short-term climate fluctuations such as the annual variance of solar radiation are implemented through Gaussian white noise. If the noise is tuned according to the time-scale matching condition, synchronized hopping (switching) between the cold and warm climate could significantly enhance the response of the earth's climate to the weak perturbations caused by modulation of orbital eccentricity of the earth [2]. While calling this mechanism stochastic resonance, B. McNamara and K. Wiesenfeld [3] correctly pointed out that this is not strictly a resonance in the sense of an increased response when a driving frequency, Ω , is tuned to a "natural frequency" of the system. There is, however, a useful analogy to resonance in that the "response" to the periodic input is maximized when some parameters, in this case the input noise, is tuned near to a certain value.

The essential ingredients for stochastic resonance consists of a bistable system, with an energetic activation barrier or more generally a form of threshold, a weak coherent input (such as periodic signal), a source of noise that is inherent in the system or that adds to the coherent input and an output which is some function of the input and the internal dynamics of the system. For the system well characterized by linear systems (dynamics) the signal to noise ratio, SNR, at the output must equal the SNR at the input, and any increase in the input noise will result in no change in the output SNR. In contrast, the signature of stochastic resonance is an increase in the output of SNR with increased input noise. Thus, the nonlinear nature of the

problem is crucial [3]. The basic mechanism for stochastic resonance is depicted in Fig. (1.1). Imagine a ball sitting in one of the two wells - let us say, a marble in an egg carton. A gentle force (periodic or aperiodic) rocks the whole system back and forth. This perturbation may be looked upon as an information carrying signal acting on a nonlinear system. Under the influence of this weak force, the ball simply rolls around in the bottom of the well. If the ball's movement is detected only when it jumps into the neighboring well, this weak signal will go unnoticed. Adding noise to the system, by tilting randomly the egg carton up and down, will, a priori, only mask the weak perturbation further. The weak signal together with the noise will allow the ball to occasionally exit into the neighboring well. Now the theory of stochastic resonance [3, 4] says that these exit events do not occur completely at random but become correlated with the weak signal. To put it more technically, an increase in noise level yields, correlated with the signal, an increase of the transition rate over the barrier into the neighboring well. On the other hand, the sensitivity of the output response decreases inversely with increasing noise level; too much noise will deteriorate the coherence for the signal assisted, noise induced exits. Thus, there does exist an optimal dose of noise upto which the addition of noise improves signal transduction. The noise enhanced output response is, therefore, fairly regular with only small fluctuations. From this perspective we find that stochastic resonance is a cooperative phenomenon in which a weak, coherent input signal entrains ambient noise.

Before coming up with an overview of quantitative measures of stochastic resonance that will be discussed in more detail in Chapter two, we present the most important theoretical tool needed for a quantitative treatment of stochastic resonance - the two

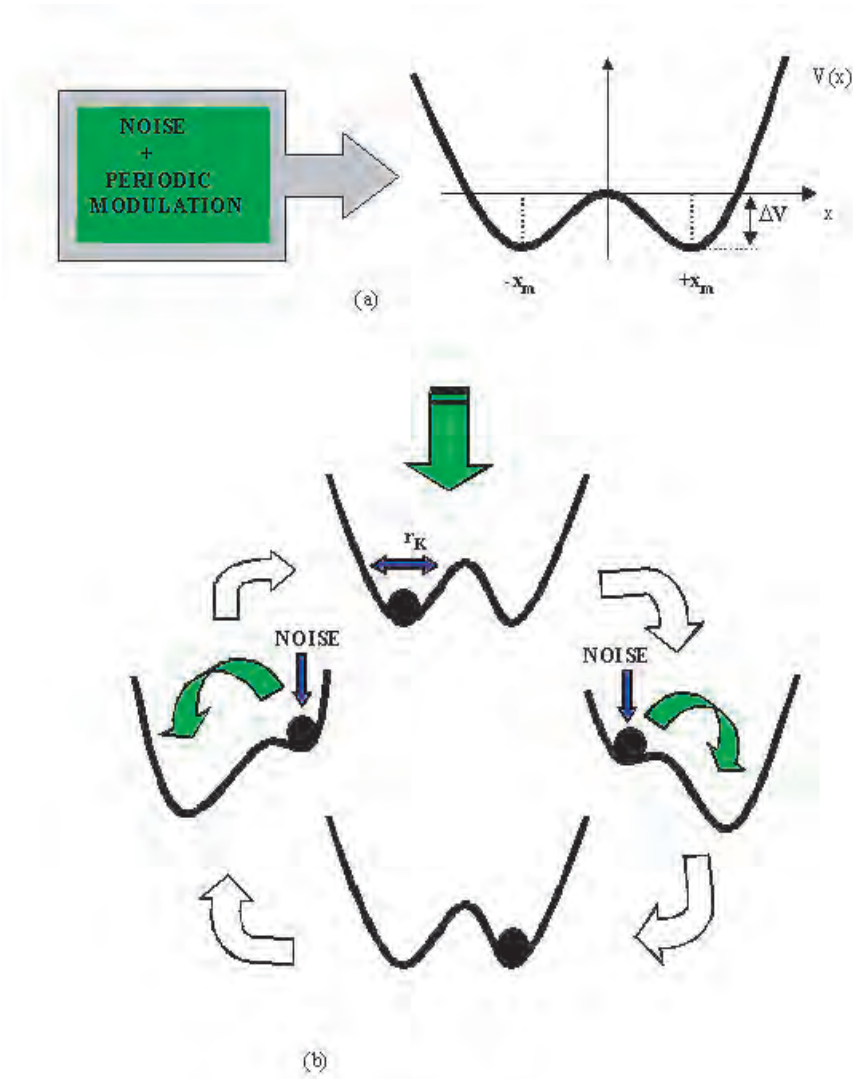


Figure 1.1: Brief illustration of the stochastic resonance mechanism

state model. We will use the two state model that in fact is general enough to constitute a great part of the many different systems analyzed in different literatures. In this model, the system resides at any time in either one of the two meta-stable states labelled 'state +' and 'state -'. Any dynamics within either states (if there is any at all) is completely neglected; we are only interested in whether the system is in state + or in state - at a given time t . Correspondingly, the output variable of the system can assume only two values:

$$x(t) = \begin{cases} +x_m & \text{in state +} \\ -x_m & \text{in state -,} \end{cases}$$

where $-x_m$ refers to the stable minimum position of the left well and $+x_m$ refers to the stable minimum position of the right well as shown in Fig. (1.1a). Such a description is possible if the time scale for the transitions between the two states is much longer than the time scale of intra-well relaxation. We furthermore assume that the system can be described in terms of two transition rates W_+ and W_- . The transition rate W_+ defines the probability that the system jumps from state - to state + while W_- defines the probability that the system jumps from state + to state - during a short time interval. In general, the transition rates depend on both the strength of the noise (more noise enhances the transition rates) and the amplitude and frequency of the external signal.

How do we measure stochastic resonance? There are various methods of measuring stochastic resonance. Some of them are the spectral characteristics of the stochastic process $x(t)$ which are the output signal and the signal-to-noise-ratio (SNR). Both of these quantities exhibit stochastic resonance if they pass through a maximum with varying noise strength. SNR is formed from the ratio of the output spectral power

at the driving frequency and the background power spectrum. Another common approach to measure stochastic resonance is the power amplification. In particular, for a periodic input signal the spectral power amplification measures [3] the ratio between the integrated spectral power of the output stored at the delta like spike of the driven power spectrum at the driving frequency and the total power of the input signal. This amplification measure undergoes a resonance like behavior: it increases with increasing noise intensity (stochastic resonance regime) until it reaches an optimal maximum and then falls off; and hence the term stochastic resonance.

In this thesis we will study stochastic resonance of a particular noise-sustained dynamics where the same noise source is used to induce the dynamics as well as the transition from mono-stable state to bistable state in order to produce a stochastic resonance under a weak periodic forcing. The rest of our work is organized as follows. In Chapter two we present general features of stochastic resonance in a double-well potential using the two-state model approach along with the definitions and derivation of the most prominent quantifiers of stochastic resonance such as spectral amplification and SNR. In Chapter three, we present our model. In the first section of Chapter three, the mechanism of converting a mono-stable potential to a bistable one is illustrated. In the next section, we present two techniques of calculating the mean first passage time, MFPT, and the corresponding transition rate. Chapter four is devoted to the result and discussion of our work and the last Chapter gives a brief summary of what has been done.

Chapter 2

General Features of Stochastic Resonance in a Bistable Potential

In the current Chapter, the general features describing the phenomenon of stochastic resonance are presented. As it has already been mentioned in the Introduction, stochastic resonance is a well established fundamental phenomenon occurring in nonlinear systems where characteristic time scales determining the system behavior can be varied by means of noise. The signature of stochastic resonance is that the coherence of the system output is improved with an increase of random noise, at least over some range of noise levels [1, 14, 17]. To fix ideas, consider the bistable double well potential of Fig. (1.1a) subjected to no noise and no periodic forcing. A heavily damped particle will come to rest at one of the two minima of the potential. In the presence of random forcing, it is well known that the particle will still spend most of its time near $\pm x_m$, but will make occasional transition over the barrier. As input noise is increased, the rate W at which such jumps will occur increases. Typically W grows very rapidly with the noise strength, D , at first, but once D is large enough that the barrier becomes relatively easy to surmount, W grows more slowly as D is further increased.

On top of this picture we add a periodic signal $A(t) = A_0 \cos(\Omega t)$ which has the effect of tilting the potential as illustrated in Fig. (1.1b). Throughout this thesis we presume that the signal amplitude, A_0 , is small enough that, in the absence of any noise, it is insufficient to force a particle to move from one well to the other. The periodic signal has the effect of modulating the transition rate, making $W_+(t)$ the rate out of the left-well, oscillate out of phase with $W_-(t)$, the rate out of the right-well. For very small noise these rates are still too slow for there to be appreciable hopping and the small periodic modulation remains important. As it has been discussed in the introduction, there are various methods of characterizing stochastic resonance. In the following sections we present some of the prominent methods of measuring (characterizing) stochastic resonance.

2.1 Characterization of stochastic resonance

Consider an over-damped motion of a Brownian particle in a bistable potential in the presence of noise and periodic forcing. The motion of the particle in double-well potential coupled to the source of noise and periodic deriving force is described by the Langevin dynamics given by:

$$m\ddot{x} + V'(x) - A_0 \cos(\Omega t + \phi) = -\gamma\dot{x} + \sqrt{2k_B T \gamma} \xi(t). \quad (2.1)$$

Here $x(t)$ is the position of the particle at time t , m is mass of the particle, \dot{x} and \ddot{x} are respectively the velocity and acceleration of the particle where as γ is the damping coefficient. The parameters A_0 , Ω refer respectively to the amplitude and frequency of the driving force and k_B is the Boltzmann's constant. $V'(x)$ is the force derived from a double well potential with its local minima and maximum located at $x = \pm x_m$ and $x = 0$ respectively, having a barrier height, ΔV , as shown in Fig. (1.1a). The

left hand side in Eq. (2.1) represents the deterministic part of the particle dynamics, while the right hand side accounts for the effect of the thermal environment. The first part of the right hand side of the Eq. (2.1) is the frictional(drag) force and is proportional to the velocity of the particle where as the second part of equation is called the random force [23, 24, 25]. The limit of large γ , high friction limit, should result in very rapid relaxation of the Eq. (2.1) to a quasi-stationary state in which $\ddot{x} \rightarrow 0$. That is, in the high friction limit, the expression in Eq. (2.1) reduces to

$$\dot{x}(t) = \frac{1}{\gamma} [-V'(x) + A_0 \cos(\Omega t)] + \sqrt{\frac{2k_B T}{\gamma}} \xi(t). \quad (2.2)$$

In this case we have eliminated the fast variable \dot{x} , which is assumed to relax very rapidly to the value given by Eq. (2.2). This procedure is the prototype of all adiabatic elimination. The basic physical assumption is that large γ force the variables governed by equations involving large γ (e.g., \dot{x}) to relax to a value given by assuming the slow variable(in this case x) to be constant. Such fast variables are then effectively slaved by the slow variables [13]. $\xi(t)$ is a Gaussian white noise of zero mean, $\langle \xi(t) \rangle = 0$, satisfying the fluctuation-dissipation relation [23, 24]

$$\langle \xi(t) \xi(0) \rangle = \delta(t). \quad (2.3)$$

In the absence of periodic forcing, the particle fluctuates around one of its local stable states with a statistical variance proportional to the noise intensity [5, 18]. Note that the only particle property which enters the characteristics of the noise is the friction coefficient γ , which may thus be viewed as the coupling strength to the environment [23]. The probability for the particle to "hop" between the potential wells is defined through noise dependent Kramer's rate

$$r_k = \frac{\sqrt{V''(x_m)|V''(0)|}}{2\pi\gamma} \exp\left(-\frac{\Delta V}{D}\right), \quad (2.4)$$

where $D = k_B T$. Weak periodic forcing of amplitude A_0 , which alone is insufficient to make the particle switching between the potential wells leads to the periodic modulation of the potential and, consequently, to that of the probability for the particle to switch. The potential wells are tilted up and down asymmetrically [1, 2, 3, 4, 5, 6] thus periodically raising and lowering the potential barriers as illustrated in Fig. (1.1b). The noise induced hopping can become then statistically synchronized with the periodic driving force. If the averaged waiting time between two inter-well hopping events, which is given by

$$T_k(D) = \frac{1}{r_k}, \quad (2.5)$$

becomes comparable with half of the period, T_Ω , of the periodic driving force, the system attains the maximum probability to switch, as the Kramer's rate is also varied with the same period. Then the synchronization takes place thus providing simple time scale matching condition [2] for stochastic resonance:

$$T_k = \frac{T_\Omega}{2}. \quad (2.6)$$

In this spirit, the time-scale matching condition with Eq. (2.5) is recast as $\Omega = \pi r_k$, provides a reasonable condition for the maximum of the response amplitude. Hence, the phenomenon of stochastic resonance can be generally interpreted as a statistical synchronization between noise induced hopping events and weak periodic driving, achieved by noise variation.

Furthermore, in the presence of periodic forcing, since the reflection symmetry of the system is broken, the mean value, $\langle x(t) \rangle$, does not vanish. This can be intuitively

understood as the consequence of the periodic biasing towards one or the other potential well. Filtering all the information about $x(t)$, except for identifying in which potential well the particle resides at time t , known as two state filtering, one can achieve a binary reduction of the two state model. The starting point for the two state model is the Master equation [3, 10] for the probabilities $n_{\pm}(t)$ of being in one of the two potential wells denoted by their equilibrium positions $\pm x_m$ i.e

$$\dot{n}_+(t) = -W_-(t)n_+ + W_+(t)n_-, \quad (2.7)$$

$$\dot{n}_-(t) = -W_+(t)n_- + W_-(t)n_+. \quad (2.8)$$

Note that $n_+(t)$ ($n_-(t)$) is the probability of being at x_+ (x_-) at time t while $W_+(t)$ ($W_-(t)$) is the transition rate from $x_-(x_+)$ to $x_+(x_-)$ at time t . The dots over n denote the derivative with respect to time. By making use of the normalization condition $n_+ + n_- = 1$, Eqs. (2.7) and (2.8) become respectively

$$\dot{n}_+(t) = -[W_-(t) + W_+(t)]n_+ + W_+(t) \quad (2.9)$$

and

$$\dot{n}_-(t) = -[W_+(t) + W_-(t)]n_- + W_-(t). \quad (2.10)$$

The solutions of these rate equations are

$$n_+(t) = g(t)[n_+(t_0) + \int_{t_0}^t W_+(\tau)g(\tau)^{-1}d\tau], \quad (2.11)$$

and

$$n_-(t) = g(t)[n_-(t_0) + \int_{t_0}^t W_-(\tau)g(\tau)^{-1}d\tau], \quad (2.12)$$

respectively, where

$$g(\tau) = \exp\left(-\int_{t_0}^{\tau} [W_+(\tau) + W_-(\tau)]d\tau\right), \quad (2.13)$$

with unspecified initial condition $n_{\pm}(t_0)$. The periodic bias toward one or the other states due to the external periodic forcing is reflected in a periodic dependence of the transition rates

$$W_+(t) = r_k \exp\left(+\frac{A_0 x_m}{D} \cos(\Omega t)\right), \quad (2.14)$$

for transition to the right well and

$$W_-(t) = r_k \exp\left(-\frac{A_0 x_m}{D} \cos(\Omega t)\right), \quad (2.15)$$

for the transition to the left well as given in [2, 3]. On assuming that the modulation amplitude is small i.e $A_0 x_m \ll D$

$$W_+(t) + W_-(t) = 2r_k \left[1 + \frac{1}{2} \left(\frac{A_0 x_m}{D}\right)^2 \cos^2(\Omega t) \dots\right]. \quad (2.16)$$

The integrals in Eqs. (2.11) and (2.12) can be performed analytically to first order in $\frac{A_0 x_m}{D}$, and are given respectively by

$$n_+(t|x_0, t_0) = \frac{1}{2} \left\{ \exp[-2r_k(t-t_0)] \left[2\delta_{x_0, x_m} - 1 - k(t_0) \right] + 1 + k(t) \right\}, \quad (2.17)$$

and

$$n_-(t|x_0, t_0) = \frac{1}{2} \left\{ 1 - k(t) - \exp[-2r_k(t-t_0)] \left[2\delta_{x_0, x_m} - 1 - k(t_0) \right] \right\}, \quad (2.18)$$

with

$$k(t) = 2r_k \left(\frac{A_0 x_m}{D} \right) \frac{\cos(\Omega t - \bar{\phi})}{\sqrt{4r_k^2 + \Omega^2}}, \quad (2.19)$$

and

$$\bar{\phi} = \arctan\left(\frac{\Omega}{2r_k}\right). \quad (2.20)$$

The quantity $n_+(t|x_0, t_0)$ should be read as the conditional probability that $x(t)$ is in the state + at time t , given that its initial state $x_0 \equiv x(t_0)$. Here the Kronecker delta

is 1 when the system is initially in the state + and 0 otherwise. We have now set the stage to compute some of the statistical quantities of the discrete process $x(t)$ to first order in $\frac{A_0 x_m}{D}$.

2.2 System response to the periodic forcing

As a result of the establishment of synchronization, the periodic component of the system's response gets amplified at some optimal noise level. To illustrate this behavior mathematically, the expression for time-dependent system response, the solution of Eq. (2.2), could be obtained by computing the mean value, $\langle x(t) \rangle$, as follows. From the definition, we have

$$\langle x(t) | x_0, t_0 \rangle = \int x P(x, t | x_0, t_0) dx, \quad (2.21)$$

where

$$P(x, t | x_0, t_0) = n_+(t) \delta(x - x_m) + n_-(t) \delta(x + x_m). \quad (2.22)$$

By employing Eqs. (2.17, 2.18, 2.19) and Eq. (2.22) into Eq. (2.21) one can, after some manipulations, obtain in the asymptotic limit, $t_0 \rightarrow -\infty$,

$$\lim_{t_0 \rightarrow -\infty} \langle x(t) | x_0, t_0 \rangle = \langle x(t) \rangle_{as} = \bar{x}(D) \cos[\Omega t - \bar{\phi}(D)], \quad (2.23)$$

where $\bar{x}(D)$ and $\bar{\phi}(D)$ represent respectively the noise dependent amplitude of the periodic component of the system response and phase lag and are given by the following approximate expressions:

$$\bar{x}(D) = \frac{A_0 x_m^2}{D} \frac{2r_k}{\sqrt{4r_k^2 + \Omega^2}}. \quad (2.24)$$

and

$$\bar{\phi}(D) = \arctan\left(\frac{\Omega}{2r_k}\right). \quad (2.25)$$

Fig. (2.1) illustrates typical behavior of the amplitude of the periodic component of the system response. As can be seen from the figure, the periodic response of the system subjected to both periodic modulation and noise can be manipulated by varying the noise intensity, D , at the system input, since the amplitude of the periodic component, \bar{x} , depends non-monotonically on the noise strength, D . At the increase of the noise the amplitude \bar{x} first increases, reaches maximum at some optimal noise intensity D_m and decreases again thus demonstrating a behavior of stochastic resonance. In view of the above presented physical picture of stochastic resonance as a phenomenon of the system output enhancement established through synchronization of noise-induced hopping with periodic driving, the value D_m attains the following physical meaning. As explained in [3, 4, 8] the noise intensity defines the probability of the system to switch from one potential well into another which is expressed by the noise dependent switching rate of the unperturbed system given by Kramer's rate r_k (see Eq. (2.4)). Starting with low intensity $D \ll D_m$ the switching events occur very rarely thus making the periodic component of the system hardly visible since the system behavior is bounded to the intra-well motion within one potential well. As the noise is increased, the random switching rate can be tuned to $D = D_m$ so as to fulfill the time scale-matching condition, Eq. (2.6). At this point the synchronization between noise induced-switching and weak periodic modulation takes place as the probability for the system to switch reaches its maximum (and the particle reaches the "best" opportunity to switch during half period of modulation that tilts the potential). The output signal becomes tightly locked with the periodic input. At the further increase of the noise, the break of synchronization sets in for the noise intensities $D \gg D_m$, for the system manages to switch many times during each

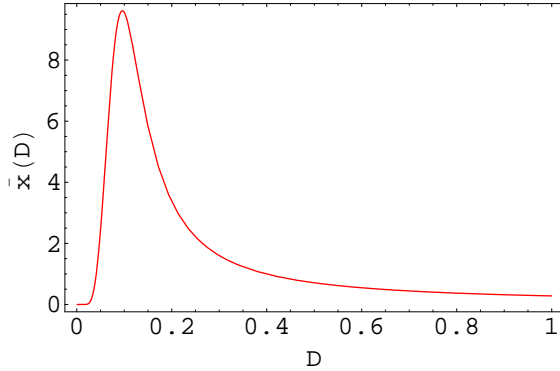


Figure 2.1: Typical behavior of the system response characteristic versus noise strength with $\Omega = 0.005\text{Hz}$, $\Delta V = 0.25\text{eV}$, $A_0 = 0.1$, and $x_m = 1$.

half of the period of the external modulation [2, 6, 18]. In Fig. (2.2), we illustrate a numerical simulation of Eq. (2.2) for single realization at three different values of noise strength, with all other parameters unchanged. To come up with this simulation (see appendix), a uniform random number ξ is generated on a digital computer at each time step. If the system is currently in the \pm state ($x = \pm x_m$), ξ is compared with the net probability, $p_{net}(t) = \Delta t W_{\pm}(t)$, of the system to jump into its neighboring state where W_{\pm} is as defined in Eqs. (2.14) and (2.15) and Δt is the time step. If the condition such that $\xi < p_{net}$ is satisfied, then the system is changed to the other state during any finite time step. What has been demonstrated in the figure goes as follows: At the lowest value of the noise level Fig.(2.2a), the average residence time in the two states is much longer than the driving period. Consequently, the individual transition occurs at unpredictable times. However, if we increase the noise level close to a particular value, we observe almost periodic transitions Fig. (2.2b): in most cases, the particle jumps from state $+$ to state $-$ and back again once per modulation period. The transitions are most likely at those instants of time when the corresponding transition rates are maximized and the average residence times in

both meta-stable states equal half the modulation period. Upon farther increase of the noise strength Fig. (2.2c), too many transitions are activated by the noise during one cycle of the periodic drive, and the cooperativity between signal and noise is lost again. This is the stochastic resonance effect: the systems response is most regular at a finite, non-vanishing noise level.

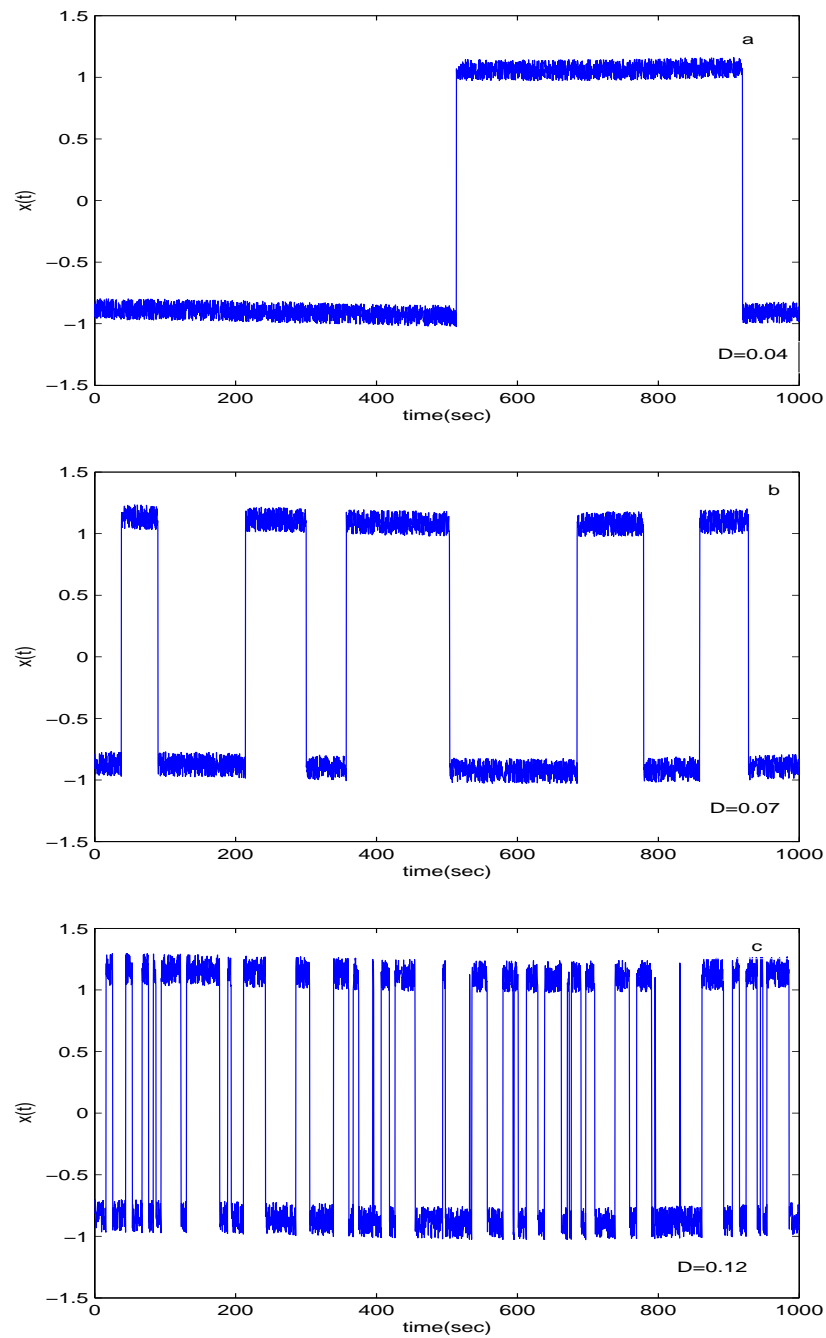


Figure 2.2: Single realization of $x(t)$ in the periodically modulated double-well potential, Eq. (2.5), with modulation amplitude $A_0 = 0.1$, modulation frequency $\Omega = 0.005\text{Hz}$, $\Delta t = 0.05\text{sec}$ and $\Delta V = 0.25\text{eV}$ for three different values of noise strength D .

2.3 The autocorrelation function

Another very essential statistical quantity that can be computed from Eq. (2.17) and Eq. (2.18) is the autocorrelation function [2]. By employing the general definition for autocorrelation function:

$$\langle x(t')x(t) | x_0, t_0 \rangle = \int \int xyP(x, t' | y, t)P(y, t | x_0, t_0)dxdy, \quad (2.26)$$

one can obtain an expression for autocorrelation function which is given by

$$\begin{aligned} \langle x(t')x(t) | x_0, t_0 \rangle &= x_m^2[2n_+(t'|x_m, t)n_+(t|x_0, t_0) + 2n_+(t' - x_m, t)n_+(t|x_0, t_0) - \\ &2n_+(t' - x_m, t) - 2n_+(t|x_0, t_0) + 1]. \end{aligned} \quad (2.27)$$

In the stationary (asymptotic) limit $t_0 \rightarrow -\infty$, Eq. 2.27 is greatly simplified, after some manipulations, to

$$\langle x(t')x(t) \rangle_{as} = x_m^2 \exp(-2r_k | \tau |)[1 - k(t)^2] + x_m^2 k(t')k(t). \quad (2.28)$$

2.4 The power spectral density

From Eq. (2.28) we can easily separate an exponentially decaying branch due to randomness and a periodically oscillating tail driven by the periodic input signal. Note that the power spectrum, which is the Fourier transform of the autocorrelation function, is a function of t as well as Ω . However in real experiments t represents the time at which one begins to take data [2, 3, 16]. Typically, one takes an ensemble of many time series at times t_1, t_2, t_3, \dots computes the power spectrum for each one, and average them together. Unless for some reason the experimenter has taken care to synchronize the phase $(\Omega t_1 - \Phi)$, $(\Omega t_2 - \Phi)$, $(\Omega t_3 - \Phi), \dots$ the values of t must properly be treated as a random variable, uniformly distributed between 0 and $\frac{2\pi}{\Omega}$. To

account for this averaging of power spectra taken at random times, one must average the power spectrum over t : $\langle S(\omega) \rangle = \frac{\Omega}{2\pi} \int_0^{\frac{2\pi}{\Omega}} S(\omega, t) dt$. Because this averaging and the Fourier transform commute (i.e becomes equal due to ergodicity), we choose to perform the averaging first, on the autocorrelation function: $\langle \langle x(t')x(t) \rangle \rangle_{as} = \frac{1}{T_\Omega} \int_0^{T_\Omega} dt \langle x(t')x(t) \rangle_{as}$ from which we can get:

$$\langle \langle x(t')x(t) \rangle \rangle_{as} = x_m^2 \exp(-2r_k |\tau|) \left[1 - \frac{1}{2} \left(\frac{A_0 x_m}{D} \right)^2 \frac{4r_k^2}{4r_k^2 + \omega^2} \right] + \frac{x_m^2}{2} \left(\frac{A_0 x_m}{D} \right)^2 \frac{4r_k^2 \cos(\Omega\tau)}{4r_k^2 + \Omega^2}. \quad (2.29)$$

Finally, the power spectrum is given by the Fourier transform of the autocorrelation function $\langle S(\omega) \rangle = \int_{-\infty}^{\infty} \exp(-i\omega\tau) \langle \langle x(t')x(t) \rangle \rangle_{as} d\tau$. Carrying out this integral we find the expression for the power spectrum to be:

$$\langle S(\omega) \rangle = \left[1 - \frac{1}{2} \left(\frac{A_0 x_m}{D} \right)^2 \frac{4r_k^2}{4r_k^2 + \Omega^2} \right] \frac{4r_k x_m^2}{4r_k^2 + \omega^2} + \frac{\pi}{2} \left(\frac{A_0 x_m}{D} \right)^2 \frac{4r_k^2 x_m^2}{4r_k^2 + \Omega^2} \left[\delta(\omega - \Omega) + \delta(\omega + \Omega) \right]. \quad (2.30)$$

From this equation one can easily observe that the expression for the power spectral density in the absence of periodic perturbation ($A_0 = 0$) reduces to

$$S(\omega) = \frac{4r_k x_m^2}{4r_k^2 + \omega^2}. \quad (2.31)$$

Naturally, the output spectral density $S(\omega)$, Eq. (2.30), of the system driven by noise and periodic modulation is represented by superposition of background noise spectral density $S_N(\omega)$ and a number of delta-like spikes centered at $\omega_n = (2n + 1)\Omega$, with $n = 0, \pm 1, \pm 2, \dots$. Considering only first harmonic for small amplitude of the external modulation signal the power spectral density of the system output can be separated into two terms: the periodic component with amplitude $\bar{x}(D)$ given by Eq. (2.24) and the noisy background $S_N(\omega)$:

$$S(\omega) = S_s(\omega) + S_N(\omega), \quad (2.32)$$

where

$$S_s(\omega) = \frac{\pi}{2} \bar{x}^2(D) \left[\delta(\omega - \Omega) + \delta(\omega + \Omega) \right], \quad (2.33)$$

and

$$S_N(\omega) = \left[1 - \frac{1}{2} \left(\frac{A_0 x_m}{D} \right)^2 \frac{4r_k^2}{4r_k^2 + \Omega^2} \right] \frac{4r_k x_m^2}{4r_k^2 + \omega^2}. \quad (2.34)$$

The noise spectrum, $S_N(\omega)$, is the product of the Lorentzian obtained with no input signal ($A_0 = 0$) and a correction factor which represents the effect of the signal on the noise. For sufficiently small signal amplitude, this factor is nearly unity. The correction factor has the effect of an overall reduction of the noise power, and this reduction is most pronounced for the signal of low frequency, $\Omega \ll r_k$, and large amplitude. The total output power, P_T , signal plus noise, is defined as the integral of the power spectrum over all frequencies given by

$$P_T = \int_{-\infty}^{\infty} d\omega S(\omega) = 2\pi x_m^2. \quad (2.35)$$

Note that P_T is independent of the input signal amplitude and frequency, Ω . Hence the effect of the input signal is to transfer power from the broad band noise into the delta spikes of the power spectral density.

2.5 Spectral power amplification

According to [2, 16] the spectral amplification is introduced on the basis of the amplitude of periodic component of the output signal as follows. The integrated power P_s of the delta like peak at an external modulation frequency $\pm\Omega$ of the output power

spectrum is

$$P_s = \int_{-\infty}^{\infty} d\omega S_s(\omega) = \pi \bar{x}^2(D). \quad (2.36)$$

In the same fashion, the total power of the modulation signal, P_A , in the absence of noise is given (as a consequence of Parseval's formula ¹) as

$$P_A = \int_{-\infty}^{\infty} A^2(t) dt = \pi A_0^2, \quad (2.37)$$

where $A(t) = A_0 \cos(\Omega t)$. The spectral amplification is defined as the ratio between P_s and P_A which is given as

$$\eta = \frac{P_s}{P_A} = \left[\frac{\bar{x}^2(D)}{A_0} \right]^2. \quad (2.38)$$

One can see from Eq. (2.38) that the power spectral amplification is independent of the input amplitude in the regime of linear response. This amplification measure undergoes a resonance like behavior: it increases with increasing noise intensity until it reaches an optimal maximum and then falls off; hence the term stochastic resonance as can be seen from Fig. (2.3).

The spectral amplification also yields a measure of synchronization between the input signal and the noise activated output dynamics. Another common approach to characterize stochastic resonance is the signal to noise ratio (SNR) whose expression can be derived in the next section.

¹Parseval's Theorem states that power computed in either domain equals the power in the other: $\int_{-\infty}^{\infty} s^2(t) dt = \int_{-\infty}^{\infty} (|S(\omega)|)^2 d\omega$ where $S(\omega)$ is the Fourier transform of $s(t)$ [26].

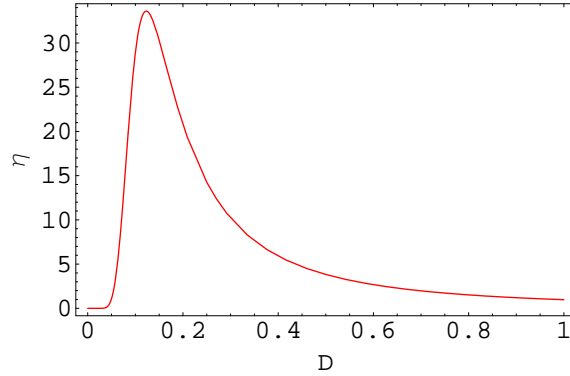


Figure 2.3: Plot of spectral power amplification versus noise strength with $\Omega = 0.005Hz$, $\Delta V = 0.25eV$, $A_0 = 0.1$, and $x_m = 1$.

2.6 Signal-to-noise-ratio(SNR)

As mentioned in the Introduction, stochastic resonance is manifested by an enhancement of weak signals by means of noise. Therefore the study of this effect can be considered as a problem of weak signal extraction from broad band background noise. SNR is a quantity which is used in engineering to describe the quality of a signal (information) within a noise background [8]. It is given by a ratio of signal output power spectral density that a delta function carries to the broad-band noise output in the presence of periodic modulation when the frequency is equal to the frequency of the periodic modulation:

$$SNR = \frac{\int_{-\infty}^{\infty} S_s(\omega)d\omega}{S_N(\omega = \Omega)} = \pi \left(\frac{A_0 x_m}{D} \right)^2 r_k \left[1 - \frac{1}{2} \left(\frac{A_0 x_m}{D} \right)^2 \frac{4r_k}{4r_k^2 + \Omega^2} \right]^{-1}. \quad (2.39)$$

By making use of Eqs. (2.33) and (2.34) the signal to noise ratio, SNR, to the leading order of $\frac{A_0 x_m}{D}$ becomes

$$SNR = \pi \left(\frac{A_0 x_m}{D} \right)^2 r_k + O(A_0^4), \quad (2.40)$$

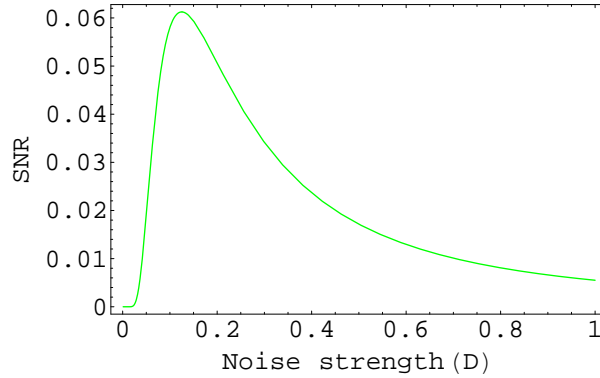


Figure 2.4: SNR as a function of noise strength with $\Omega = 0.005\text{Hz}$, $\Delta V = 0.25\text{eV}$, $A_0 = 0.1$, and $x_m = 1$.

for $\frac{A_0 x_m}{D} \ll 1$. Note that the noise intensity \bar{D}_{SR} at which SNR assumes its maximum (Fig. (2.4)) doesn't coincide with the value D_m that maximize the response amplitude (Fig. (2.1)), $\bar{x}(D)$, or equivalently the strength of the delta spike in the power spectrum given by Eq. (2.33). As a matter of fact, if the pre-factor of the Krammer's rate is independent of D , we find that the SNR of Eq. (2.40) has a maximum at $\bar{D}_{SR} = \frac{\Delta V}{2}$.

Upto now we have been discussing general theoretical background of the phenomenon of stochastic resonance alongwith the basic definitions and derivations of some of the fundamental observables of stochastic resonance such as spectral amplification and SNR. Now that we have established the ideas of stochastic resonance, we can present a framework of our particular model system with a specific source of noise, unlike what has been discussed previously, employing a numerical technique in the next Chapter.

Chapter 3

Stochastic resonance due to thermally induced noise in bistable system

Stochastic resonance is a nonlinear effect wherein the noise turns out to be beneficial to the transmission or detection of an information carrying signal as explained in the introduction part. This paradoxical effect has now been reported in a large variety of nonlinear systems, including electronic circuits, optical devices, neuronal systems, chemical reactions, etc [5]. Stochastic resonance can take place under various forms according to the types considered for the noise, for the information carrying signals, for the nonlinear systems realizing the transmission or detection, and for the quantitative measure of performance receiving improvement from the noise.

In this Chapter, we consider a particular system which undergoes noise-assisted transition from a mono-stable state to a bistable under certain conditions. When a periodic signal which has the effect of rocking the potential is added to the system under bistable state, the system exhibits the dynamics that is found to manifest stochastic resonance. We utilize the methods discussed in the pervious Chapter that enable us to determine the transition rate between the neighboring stable states. This leads us

to exploring the various features of stochastic resonance such as output signal, output noise, signal-to-noise-ratio and power amplification as a function of a particular parameter. In the first section we will present the model system and the dynamics governing it. Further, we will set the region in which bistability is maintained. Finally, two different approaches for calculating the mean first passage time and the corresponding transition rate that are repeatedly used in the next Chapter will be presented.

3.1 Impurity diffusion in a non-homogeneous temperature

The correct form of the diffusion equation in the case of an inhomogeneous medium, whose temperature may also vary in space, has been the subject of some debates [9, 11]. However, a number of special models, amenable to explicit computation, have been investigated. For our purpose here, we prefer to employ a hopping model alongwith an inhomogeneous temperature and properties of a medium containing a uniformly located traps on all lattice sites. For simplicity, we consider motion of a particle to be in one dimension, which will be measured on the macroscopic scale by x . On top of this picture, consider the particle hopping from one trap to the next where the time spent between each traps being negligible. This process constitutes a continuous time random walk, provided that the particle spends enough time in each trap for any memory of its preceding adventures to be erased by the thermal motion of the lattice.

Suppose that each trap consists of a pit in the internal potential of depth Φ . Having surmounted the energy trap, Φ , the particle will travel either to the left or to the

right until it meets another trap. Suppose the particle moving in the energy trap of the medium, Φ , is also subjected to an external potential, $V(x)$, which is produced by certain sources (e.g split-gates [22]) in a space-dependent temperature background, $T(x)$. Assuming that the traps are homogenously distributed and the impurity density is low enough to neglect the effect of impurity-impurity (Coulomb) interaction throughout, the dynamics for the population density is [11, 12] governed by

$$\frac{\partial P(x, t)}{\partial t} = \frac{\partial}{\partial x} \left[\frac{V'(x)}{k_B T(x)} \exp\left(-\frac{\Phi}{k_B T(x)}\right) P(x, t) + \frac{\partial}{\partial x} \left(\exp\left(-\frac{\Phi}{k_B T(x)}\right) P(x, t) \right) \right], \quad (3.1)$$

where $P(x, t)$ is the impurity probability density at position x and time t . In our model, we take a one dimensional system in which particles hop from one trap to the next assisted by thermal noise. If the external potential is mono-stable, the particles will be piled in the potential minimum governed by the Boltzmann's distribution factor $\exp\left(\frac{-V(x)}{k_B T}\right)$ provided that the background temperature is uniform. If, however, the temperature of the medium is non-homogenous (the case we are going to consider below) the impurity distribution no longer obeys the Boltzmann's distribution as the system is out of equilibrium [21]. Hence, the type of the temperature profile we consider here so that the particles will be piled into two stable points instead of one potential minimum is a non-uniform one which falls exponentially to the cold background temperature given by

$$T(x) = T_C + T_H \exp\left(-\left(\frac{x}{\sigma}\right)^2\right). \quad (3.2)$$

The effect of non-uniformity in the temperature on the way the impurities diffuse leads to a different distribution in the probability whose value is determined globally. To put it more technically, a locally hot region somewhere along x can cause the particles to be most likely at places totally different from that of the initial potential

minimum. On the other hand, we take the position dependent external potential to be a parabolic of the form

$$V(x) = V_0 \left(\frac{x}{\mu} \right)^2, \quad (3.3)$$

that controls the diffusion of the impurities. The impurities without the external potential have equal chance to hop in all directions. The potential is used to bias the hopping towards lower potential, the minimum energy point being the minimum of the external parabolic potential [22]. The two quantities σ and μ characterize respectively the spatial length scale of the excess hot temperature and the amount by which the external potential varies along the lattice sites. We set a comparison between them in the form

$$\sigma = n\mu, \quad (3.4)$$

where the values of n can be fixed in such a way that the system stays in the bi-stabile region. A proper explanation of the parameter σ would require us to delve into radiation (light) from a laser beam one may essentially need to use in order to heat-up the mono-stable potential under consideration from the bottom so that it will be converted to a bistable system. Thus, this parameter may also be considered as the width of the laser beam's radiation (light) covering certain length of the material being heated.

So far, it has been reported in [10] that the phenomenon of stochastic resonance can be manifested as a function of T_C when T_H is fixed to certain value; where they actually set the quantities characterizing the spatial length of the excess temperature σ and the amount by which the external potential varies along the lattice site μ exactly identical. In this thesis, however, we study the phenomenon of stochastic resonance as a function of hot temperature for different values of the parameter n connecting σ

and μ as in Eq. (3.4) by setting T_C to room temperature, ($T_C = 300K$).

Now that we have established a bistable potential by assuming the density of impurities to be very small such that the Coulomb-Coulomb interaction is neglected, we can add up the whole impurities into one and consider it as a Brownian particle. The steady-state probability distribution of the particle, $P_{ss}(x)$, can be obtained from Eq. (3.1) as

$$P_{ss}(x) = C \exp\left(-\frac{V_{eff}(x)}{k_B T_C}\right), \quad (3.5)$$

where C is the normalization constant and $V_{eff}(x)$ is the effective potential which is given by

$$V_{eff}(x) = V_0 \left(\frac{x}{\mu}\right)^2 + V_0 \left(\frac{\sigma}{\mu}\right)^2 \ln\left(\frac{T_C}{T_H} + \exp\left(-\left(\frac{x}{\sigma}\right)^2\right)\right) + \frac{\Phi}{1 + \frac{T_C}{T_H} \exp\left(\frac{x}{\sigma}\right)^2} - U_0, \quad (3.6)$$

with

$$U_0 = \Phi + V_0 \left(\frac{\sigma}{\mu}\right)^2 \ln\left(1 + \frac{T_C}{T_H}\right). \quad (3.7)$$

It is essential to note here that the expression for steady-state probability distribution, Eq. (3.5), is equivalent to converting the non-equilibrium problem to equilibrium one in which the usual Boltzmann statistics holds. In Fig. (3.1), we illustrate how the effective potentials behave as a function of position for different values of hot temperatures and the parameter n . Note that the shape of the effective potentials is controlled by the parameters T_C , T_H , Φ , n , and V_0 . The effective potential corresponding to the system with $n = 0.5$ exhibits a quicker transition from mono-stable to bistable than the system with $n = 1.0$. In other words, the minimum hot temperature for the transition to take place is nearly 8K for $n = 0.5$ while it is 35K for $n = 1.0$. Therefore, to rephrase it more technically, reducing the values of the parameter n to, for example, $n = 0.5$ results in an unambiguous double stable potential profiles even

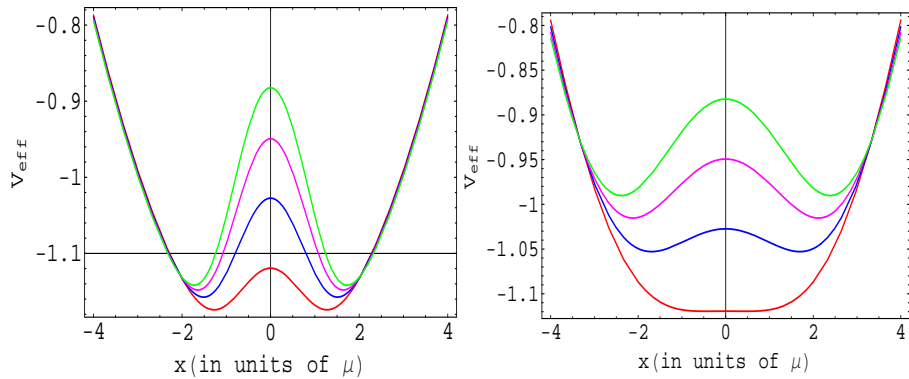


Figure 3.1: Plots of effective potentials as a function of position for $T_H = 35K$, $65K$, $95K$, $125K$ from bottom to top with $T_C = 300K$, $\mu = 5.43nm$, $V_0 = 0.125eV$, $\Phi = 10V_0$, $n = 0.5$ (left), $n = 1.0$ (right).

for small T_H when compared with the profiles for the case $n = 1.0$.

We ask: what effects do (on both plots) increasing T_H has on the barrier height, ΔV , and the width between the stable points? Close observations of Fig. (3.1) can provide the answer, although not conclusive answer, to this question. As it can be seen from the plots, increasing the temperature T_H increases simultaneously the potential barriers, ΔV , and the distances between the two minima of the potential functions, for whatever values of the parameter n . For a very large values of T_H , the particle moving in the equivalent bistable system can hardly jump over the potential barrier since the height, ΔV , of the potential gets too high. So the particle dances in one of the two potential wells, the output signal is very small and the SNR will be very low, though the effect is more pronounced for the system with $n = 0.5$. When the temperature is relatively low, however, the small ΔV makes the particle easy to jump between the two wells, the output signal can thus be improved, at least in some range of T_H , and the signal to noise ratio (SNR) increases. Therefore, there exist some values of T_H for which the signal to noise ratio, SNR, reaches its maximum value. In

other words, the SNR is a non-monotonic function with T_H for both the system with $n = 1.0$ and $n = 0.5$. On the other hand, the potential barrier, ΔV , is observed to be monotonically increasing function of T_H in both cases.

From Eq. (3.6) one can easily obtain the range in which the bistability will be maintained. This is done by first setting the first derivative with respect to x of V_{eff} , Eq. (3.6), to zero and solving for x .

$$\frac{dV_{eff}}{dx} = 0, \quad (3.8)$$

from which we obtain

$$x = 0, \quad (3.9)$$

and

$$x = \pm \sigma \sqrt{\ln \left[\left(\left(\frac{\mu}{\sigma} \right)^2 \frac{\Phi}{V_0} - 1 \right) \frac{T_H}{T_C} \right]} = \pm x_m. \quad (3.10)$$

Eqs. (3.9) and (3.10) are referred respectively as the unstable and stable points of the dynamics. From Eq. (3.10) we observe that the bistability will be maintained provided that the argument in the logarithm is greater than unity i.e

$$\left(\left(\frac{\mu}{\sigma} \right)^2 \frac{\Phi}{V_0} - 1 \right) \frac{T_H}{T_C} > 1. \quad (3.11)$$

Based on this inequality one can easily fix the values for T_H , T_C and n so that the bistability is maintained. Otherwise, when $\left(\left(\frac{\mu}{\sigma} \right)^2 \frac{\Phi}{V_0} - 1 \right) \frac{T_H}{T_C} \leq 1$ the system will turn out to be mono-stable. One can easily observe that the system changes from a mono-stable potential to a bistable one and the transition point in the parameter space occurs when

$$\frac{T_H}{T_C} = \frac{V_0}{\left(\frac{\mu}{\sigma} \right)^2 \Phi - V_0}. \quad (3.12)$$

Note that we are considering a particular material, silicon carbide with traps on each lattice sites, whose separation between consecutive sites is $0.543nm$ [22] and having some impurities, in a given background temperature; i.e μ , Φ , T_C are fixed. Evidently, the transition of the state from mono-stable to bistable one depends on the strength of the hot temperature considered. The temperature intensity supplies the random kicks that enables the impurities to diffuse away from the center by making it unstable. This unstable point corresponds to $x = 0$ where as the new places where the impurities diffuse to correspond to the two stable points $x = \pm x_m$ of Fig. (1.1a). Evaluating the effective potential, V_{eff} at $x = 0$ and at $x = \pm x_m$, the two local maximum and minima, one can get the height, ΔV , of the potential barrier as

$$\Delta V_{eff} = \frac{\Phi}{1 + \frac{T_C}{T_H}} + V_0 \left(\frac{\sigma}{\mu} \right)^2 \ln \left[\left(1 + \frac{T_C}{T_H} \right) \left(\frac{\sigma}{\mu} \right)^2 \frac{V_0}{\Phi} \right] - V_0 \left(\frac{\sigma}{\mu} \right)^2. \quad (3.13)$$

Up to now, we have formulated the effective potential, the conditions under which bistability is maintained and the expression for the barrier height. As long as the potential barrier exists, the particle put in either of the two states "hops" to the neighboring state under certain favorable conditions. In the following section we will present the concept of both the mean first passage time and the corresponding transition rate whereby two methods of computing them numerically, namely high barrier limit and exact numerical techniques are developed.

3.2 Mean first passage time and escape rate

In the following, we will be interested only in those transition events not in the motion within either potential well("intra-well motion"). The plan is to numerically evaluate the double integral of Eq. (3.16) below assuming the system starts at the left minimum $x = -x_m$ and is absorbed at the right minimum $x = +x_m$.

We ask: If a particle is initially placed at the left minimum, $x = -x_m$, how long will it take for the particle to reach the right minimum, $x = +x_m$, for the first time? The answer will vary from realization to realization, and we call the expectation value the "mean first passage time". Consider that the system under investigation is subjected, in the adiabatic limit, when the signal frequency is much slower than some relaxation time, to a time periodic signal $A(t) = A_0 \cos(\Omega t)$ [3]. The potential of the system is then modulated by the periodic signal and is given as

$$V(x, t) = V_{eff}(x) - A_0 x \cos(\Omega t) \quad (3.14)$$

where A_0 and Ω are, respectively, the periodic signal amplitude and frequency. The quasi-steady state distribution function $P_{ss}(x, t)$ corresponding to Eq. (3.1) can then be modified as

$$P_{ss}(x, t) = C \exp \left[- \frac{V_{eff}(x) - A_0 x \cos(\Omega t)}{k_B T_C} \right] \quad (3.15)$$

where C is the normalization constant. In order to calculate the transition(escape) rate out of $+(-)x_m$ states, we first calculate the mean first passage time for the particle to reach the states $-(+x_m)$ or viceversa and then take its inverse to get the transition rate. For simplicity, assume that the particle starts from the state " - " and is given [13] by

$$T(-x_m \rightarrow x_m) = \frac{\gamma}{k_B T_C} \int_{-x_m}^{x_m} \frac{dx}{\exp \left(\frac{-V(x, t)}{k_B T_C} \right)} \int_{-\infty}^x dy \exp \left(\frac{-V(y, t)}{k_B T_C} \right) \quad (3.16)$$

This equation is not easily solvable analytically. As a result, we make use of the high barrier limit and the exact numerical method approaches to calculate for the mean first passage time and the transition rate by considering the cases where $n = 1.0$ and $n = 0.5$.

3.2.1 The high barrier limit approach

If the central maximum of $V(x, t)$, Fig. (1.1b), is large compared to $k_B T_C$, i.e $\Delta V \gg k_B T_C$, the region where Kramer's rate holds, then $\exp \left[\frac{V(x, t)}{k_B T_C} \right]$ is sharply peaked at $x = 0$, an unstable point, while $\exp \left[-\frac{V(y, t)}{k_B T_C} \right]$ is very small near $y = 0$. Therefore, $\int_{-\infty}^x dy \exp \left[-\frac{V(y, t)}{k_B T_C} \right]$ is very slowly varying function of x near $x = 0$. This means that the value of the integral $\int_{-\infty}^x dy \exp \left[-\frac{V(y, t)}{k_B T_C} \right]$ will be approximately constant for those values of x which yield a value of $\exp \left[\frac{V(x, t)}{k_B T_C} \right]$ which is significantly different from zero. Hence in the inner integral, we can set $x = 0$ and remove the resulting constant factor from inside the integral with respect to x . Measuring the mean first passage time of Eq. (3.16) in the units of the damping coefficient, γ , we obtain:

$$\langle \tau \rangle = \frac{1}{k_B T_C} \left\{ \int_{-\infty}^0 dy \exp \left(-\frac{V(y, t)}{k_B T_C} \right) \right\} \left\{ \int_{-x_m}^{x_m} \frac{dx}{\exp \left(\frac{-V(x, t)}{k_B T_C} \right)} \right\}. \quad (3.17)$$

Employing Eq. (3.14) into Eq. (3.17) we find an approximation for the mean first passage time out to be

$$\langle \tau \rangle = \frac{1}{k_B T_C} \left\{ \int_{-\infty}^0 dy \exp \left(-\frac{V_{eff}(y) - A_0 y \cos(\Omega t)}{k_B T_C} \right) \right\} \left\{ \int_{-x_m}^{x_m} \frac{dx}{\exp \left(-\frac{V_{eff}(x) - A_0 x \cos(\Omega t)}{k_B T_C} \right)} \right\}. \quad (3.18)$$

As it has been discussed in Chapter two, the stochastic resonance quantifiers are a function of escape rate r_k obtained in the absence of the rocking force ($A_0 = 0$). Hence, we must be able to calculate the escape rate by setting $A_0 = 0$ in Eq. (3.18) that can be reduced to:

$$\langle \tau \rangle = \frac{1}{k_B T_C} \left\{ \int_{-\infty}^0 dy \exp \left(-\frac{V_{eff}(y)}{k_B T_C} \right) \right\} \left\{ \int_{-x_m}^{x_m} \frac{dx}{\exp \left(-\frac{V_{eff}(x)}{k_B T_C} \right)} \right\}. \quad (3.19)$$

Since this equation is not easily solvable analytically, we make use of a numerical technique, Simpson's 1/3 rule [20], to calculate the approximate mean first passage time and the corresponding transition rate after substituting Eq. (3.6) into Eq. (3.19).

3.2.2 The exact numerical technique

In the previous subsection we have formulated the approximate methods of computing the mean first passage time and the transition rate of a particle moving from one well to the other under the assumption of a high barrier limit. For the sake of comparison, we will calculate the exact values of mean first passage time and the corresponding escape rate. As stated in Eq. (3.16), the expression for the mean first passage time, in a high friction limit, is

$$\langle \tau \rangle = \frac{1}{k_B T_C} \int_{-x_m}^{x_m} \frac{dx}{\exp\left(\frac{-V(x,t)}{k_B T_C}\right)} \int_{-\infty}^x dy \exp\left(\frac{-V(y,t)}{k_B T_C}\right). \quad (3.20)$$

In the absence of periodic force, Eq. (3.20), will be simplified into:

$$\langle \tau \rangle = \frac{1}{k_B T_C} \int_{-x_m}^{x_m} \frac{dx}{\exp\left(\frac{-V_{eff}(x)}{k_B T_C}\right)} \int_{-\infty}^x dy \exp\left(\frac{-V_{eff}(y)}{k_B T_C}\right). \quad (3.21)$$

Here also we make use of the Simpson 1/3 rule method [20] to integrate each integrals without taking any assumption unlike the case of high barrier limit approach. Note that all the results of our discussion in this section will be presented in the next Chapter.

Chapter 4

Result and discussion

In Chapter two we derived expressions for different quantities which are eminently invoked to quantify stochastic resonance. These expressions are obtained as a function of escape rate which is also discussed through numerical approach in the previous Chapter. In the current Chapter, we are interested in analyzing the quantitative aspect of those quantifiers by employing the numerical results of the escape rate discussed in both exact and approximate numerical technique in Chapter three.

The effective dynamics of the system, as discussed in the previous Chapter, exhibits bistability only in the range $\left[\left(\frac{\mu}{\sigma}\right)^2 \frac{\Phi}{V_0} - 1\right] \frac{T_H}{T_C} > 1$. Therefore, to fix our parameters in this range, we set $T_C = 300K$, $k_B = 86.17\mu eV$, $\mu = 5.43nm$, $\Phi = 10V_0$ and $V_0 = 0.125eV$ throughout this Chapter. Before coming up with the analysis of the quantitative measures of stochastic resonance, we present the results of our discussion in sections 3.1.2 and 3.1.3 through Fig. 4.1 and 4.2.

Fig. (4.1) demonstrates the plots of the exact and approximate mean first passage time of the system under investigation versus hot temperature for two values of the parameter n . As it can be seen from the plots, the exact calculation is in perfect qualitative agreement with the approximate calculation. The two plots show that

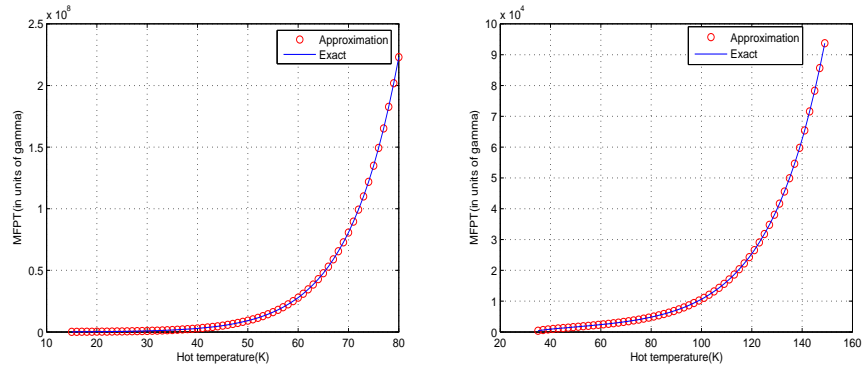


Figure 4.1: Exact and Approximate values of mean first passage time as a function of hot temperature for $n = 0.5$ (left) and $n = 1.0$ (right).

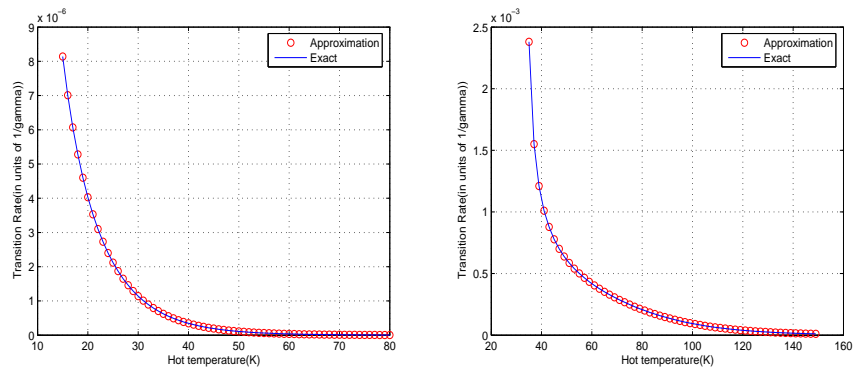


Figure 4.2: Exact and Approximate values of Transition rate versus hot temperature for $n = 0.5$ (left) and $n = 1.0$ (right).

the particle takes relatively longer time to hop the barrier as the temperature rises than it does in the lower hot temperature region. As the temperature is increased, the particle is confined only to intra-well motion because it is unable to surmount the larger barrier created. This means that the particle, in going over the barrier to the right or to the left well, takes most of the time in actually surmounting the barrier. It is worth to note also that the particle stays much time in the same well in the case of $n = 0.5$ than it does in the case of $n = 1.0$ as it can be seen from Fig. (4.1). This is true because the barrier height is larger in the first case than it is in the later case(see Fig. (3.1)). On the other hand, Fig. (4.2) demonstrates that the particle attains the maximum transition rate in the relatively lower hot temperature regime. Furthermore, the particle attains large transition rate when $n = 1.0$ than when $n = 0.5$ as in Fig. (4.2). In the next sections, we repeatedly employ the values of these transition rates .

4.1 Amplitude of the periodic response

As a result of a synchronization establishment, the periodic component of the system response gets amplified at some optimal noise level. Referring to Eq. (2.24), the amplitude of the periodic component of the system response due to the modulation is given as

$$\bar{x} = \frac{A_0 x_m^2}{k_B T_C} \frac{2r_k}{\sqrt{4r_k^2 + \Omega^2}}. \quad (4.1)$$

Fig. (4.3) is used to demonstrate the plot of Eq. (4.1) as a function of hot temperature for two different values of n: $n = 1.0$ and $n = 0.5$.

At a closer inspection of Fig. (4.3), we note that the amplitudes first increases with increasing the hot temperature, reach a maximum and then decrease again. This

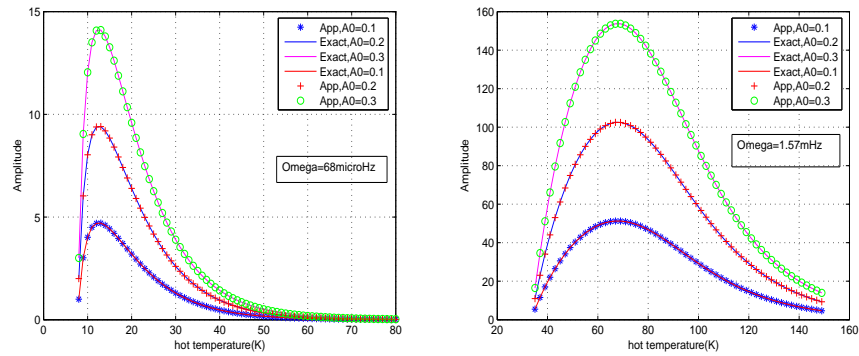


Figure 4.3: Amplitude of a periodic component of the system response versus hot temperature at a fixed periodic frequency, Ω , for different values of periodic amplitude with $n = 0.5$ (left) and $n = 1.0$ (right).

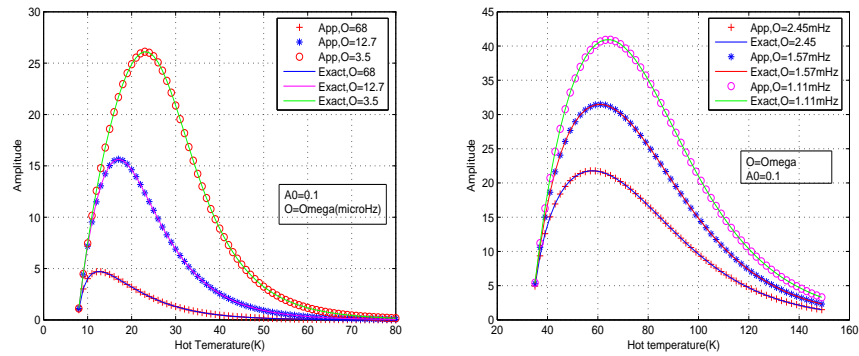


Figure 4.4: Amplitude of a periodic component of the system response as a function of hot temperature at a fixed modulation amplitude of $A_0 = 0.1$ for different values of deriving frequency with $n = 0.5$ (left) and $n = 1.0$ (right).

is the celebrated stochastic resonance effect. On the one hand, it is important to note that the amplitude \bar{x} increase monotonically with the increase of the amplitude A_0 of the rocking force in both cases. On the other hand, Fig. (4.4) illustrates that \bar{x} of the periodic response decreases monotonically with the increase in the frequency of the signal. This point illustrates that stochastic resonance phenomenon requires a low deriving frequency to occur.

4.2 Spectral amplification

The spectral amplification is one of the most prominent characteristics used to demonstrate the effect of the amplification of the output signal at the variation of the noise intensity. To characterize the behavior of the spectral amplification in dependence of system parameter Ω , we produce the numerical solution of the equation:

$$\eta = \left[\frac{x_m^2}{k_B T_C} \frac{2r_k}{\sqrt{4r_{k2} + \Omega^2}} \right]^2 \quad (4.2)$$

Fig. (4.5) shows the spectral amplification evaluated for three different frequencies as a function of hot temperature with $n = 0.5$. It can be seen that for high frequency Ω the dependence is almost flat and there is practically no power amplification present. At the decrease of the frequency of the modulation signal, the maximal value of spectral amplification grows. The position of the maximum shifts towards lower hot temperature values as Ω increases. Generally, the spectral amplification in this case shows the behavior of monotonically decreasing function.

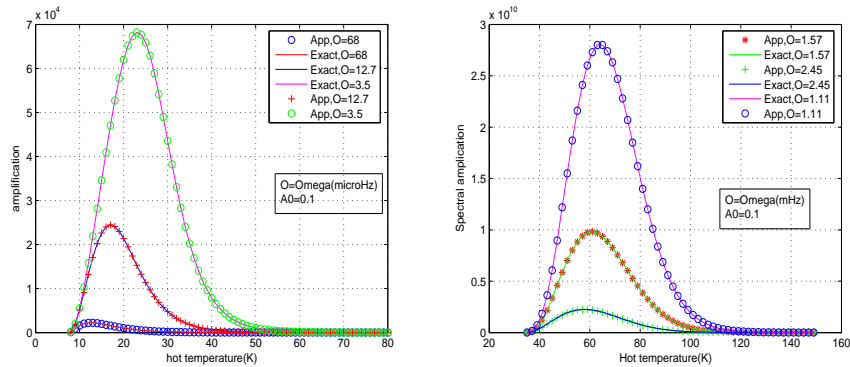


Figure 4.5: Spectral Amplification as a function of hot temperature for different values of the periodic frequency and $n = 0.5$ (left) and $n = 1.0$ (right).

4.3 Signal output power

The signal output power, as explained in Chapter two, is a Delta function at a periodic modulation frequency. i.e

$$S_s(\omega) = \pi \left[\frac{A_0 x_m^2}{k_B T_C} \frac{2r_k}{\sqrt{4r_k^2 + \Omega^2}} \right]^2 \quad (4.3)$$

In Fig. (4.6) we illustrate the signal output power versus hot temperature at a fixed modulation frequency and different values of periodic amplitude for $n = 0.5$ and $n = 1.0$. We observe from the figure that the signal output of the system also undergoes a resonance like behavior as a function of the hot temperature. One can observe from the figure that the signal output is larger for the system with $n = 1.0$, as it would be, than it does in the case $n = 0.5$, because the barrier that the system must surmount is by far larger in the later case as explained in Chapter three.

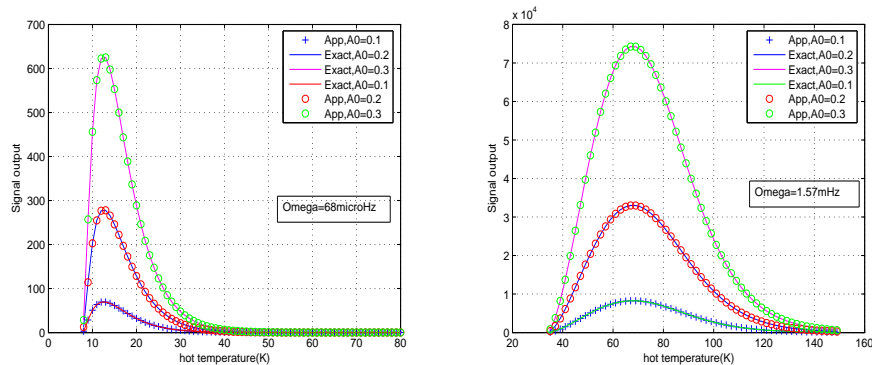


Figure 4.6: Signal output power as a function of hot temperature for $n = 0.5$ (left) and $n = 1.0$ (right) with different values of periodic amplitude.

4.4 Noise output power

In view of Eq. (2.34), one can see that the noise spectrum is the product of the Lorentzian obtained with no signal and a correction factor which represents the effect of the signal on the noise. It is given at the periodic frequency as:

$$S_N(\omega) = \left[1 - \frac{1}{2} \left(\frac{A_0 x_m}{k_B T_C} \right)^2 \frac{4r_k^2}{4r_k^2 + \Omega^2} \right] \frac{4r_k x_m^2}{4r_k^2 + \Omega^2} \quad (4.4)$$

For sufficiently small signal amplitude, the correction factor is nearly unity. This correction factor has the overall reduction of the noise power, and this reduction is most pronounced when the signal is of low frequency and large amplitude. The effect of the signal is to transfer power from the broad-band into the Delta function spike. As shown in Fig. (4.7), the noise output also exhibits a resonance-like behavior as a function of hot temperature.

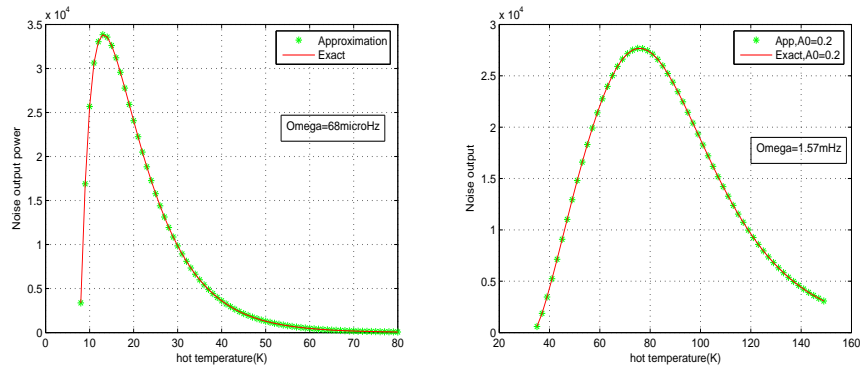


Figure 4.7: Noise output power versus hot temperature for fixed value of periodic amplitude and $n = 0.5$ (left) and $n = 1.0$ (right).

4.5 Signal-To-Noise-Ratio

Another frequently used characteristic of stochastic resonance is signal-to-noise-ratio (SNR), which is an alternative measure of signal enhancement. Traditionally, this ratio is defined as a ratio between signal output power and the noise output power at a signal frequency, as we have discussed in the pervious Chapters, and is given as:

$$SNR = \pi \left[\frac{A_0 x_m^2}{k_B T_C} \right]^2 r_k \left[1 - \frac{1}{2} \left(\frac{A_0 x_m}{k_B T_C} \right)^2 \frac{4r_k}{4r_k^2 + \Omega^2} \right]^{-1} \quad (4.5)$$

The plot of the numerical solution of Eq. (4.5) is illustrated in Fig. (4.8). As it can be seen from the figure increasing the hot temperature makes the SNR undergo a simple resonance-like dependence at an exactly single maximum point reached at some optimal hot temperature in the case of $n = 0.5$ unlike that of the case $n = 1.0$ where well defined maximum point reached is not a single point as can be seen from Fig. (4.8). It is worth to mention also that SNR a monotonic function of the periodic amplitude in both cases. In Fig. (4.9) we show the effect of periodic frequency, Ω ,

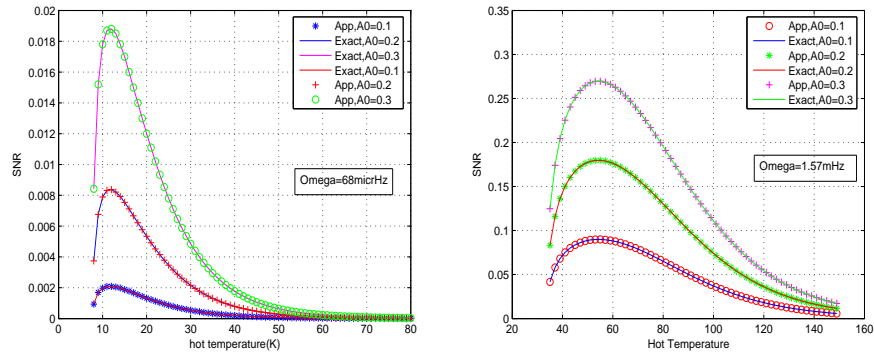


Figure 4.8: SNR as a function of hot temperature for $n = 0.50$ (left) and $n = 1.0$ (right) with different modulation amplitude.

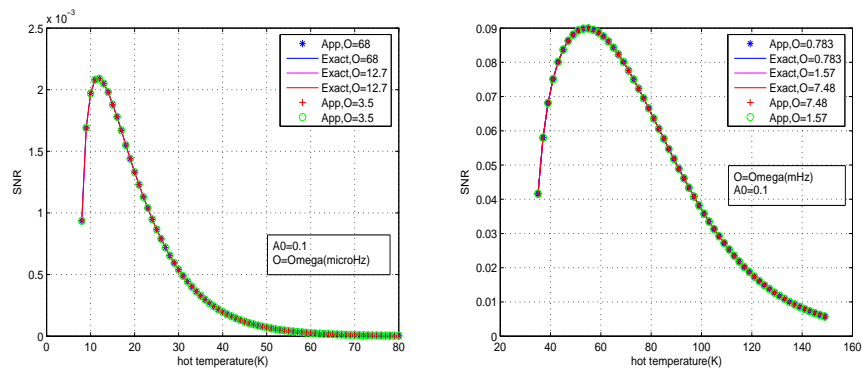


Figure 4.9: SNR for the case of $n = 1.0$ as a function of Hot temperature for different values of Ω and $A_0 = 0.1$ with $n = 0.5$.(left) and $n = 1.0$ (right)

on signal-to-noise -ratio at amplitude $A_0 = 0.1$. From the figure we can see that the effect of frequency of the input signal on the SNR is so little that there is almost no variation for different values of Ω .

Finally, in Fig. (4.10), we present the SNR, and η , as a function of the hot temperature for three different values of the parameter n with $A_0 = 0.1$ and $\Omega = 68 \mu\text{Hz}$. The existence of the maximum in these curves is still the identifying characteristics of the stochastic resonance phenomenon. It is shown that the peak points of the SNR and spectral amplification shift toward the higher hot temperature while their amplitude

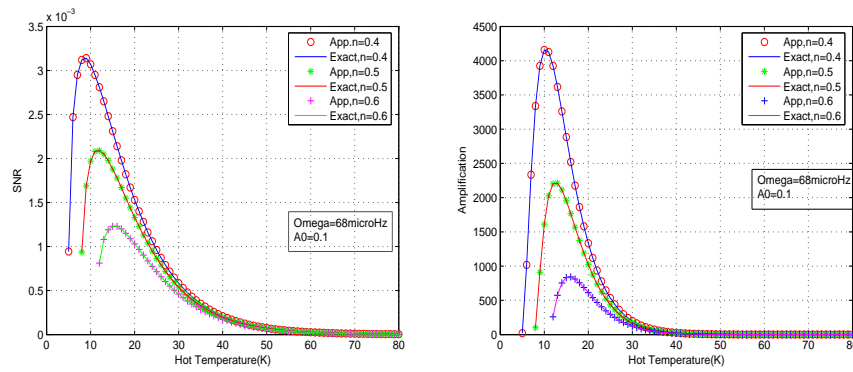


Figure 4.10: SNR (left) and spectral amplification (right) as a function of Hot temperature for different values of the parameter n with $A_0 = 0.1$ and $\Omega = 68 \mu\text{Hz}$.

fall as the values of the parameter n increase as shown in Figs. (4.10).

Chapter 5

Summary And conclusion

In this work, we first considered an over-damped motion of a Brownian particle coupled with a weak but periodic driving force and the thermal fluctuation in a bistable potential. Here, the periodic driving and the thermal fluctuation play the role of signal and noise, respectively, while the transition from one well to the other determine the output. The particle dynamics within the single well (intra-well motion) is not considered because in most cases the hopping between the wells (inter-well motion) has more physical relevance (e.g the transition between ice and warm ages) as explained in [2, 14]. After introducing the common definition, the basic underlying physical mechanisms along with the methods of characterization of the effect of stochastic resonance have been presented. Then we briefly illustrated the mechanism of stochastic resonance and the condition of input/output synchronization. Based on our formalism, we computed some of the statistical quantities characterizing stochastic resonance such as system response to the periodic forcing, power spectral density and signal-to-ratio. Also we have successfully converted a mono-stable potential into a bistable one by fixing some of our parameters as explained in the pervious Chapters. Finally, we went briefly through the discussion of mean first passage time and the

corresponding escape rate which we repeatedly used in the numerical analysis of the stochastic resonance quantifiers. The effect of stochastic resonance has been established numerically as a function of hot locality (hot temperature) in a bistable potential. The main results expected and obtained in our work for both $n = 1.0$ and $n = 0.5$ can be summarized generally as follows:

1. The stochastic resonance appears as an effect of synchronization between weak input periodic force and noisy system output resulting in the enhancement of the periodic component of the system response (observed through spectral amplification and signal-to-noise ratio.)
2. The corresponding measures of the output signal optimization such as spectral amplification and signal-to noise-ratio under go pronounced resonance -like dependence as a function of hot locality(hot temperature). But the values of hot temperature which maximizes the response amplitude and SNR don't coincide.
3. The dependence of stochastic resonance quantifiers on the amplitude of the modulation are characterized by the increase of the maximum values of the amplification and signal-to-noise -ratio at the increase of the amplitude.
4. Spectral amplification and the amplitude of the periodic response reach greater values when registered at lower frequencies of the periodic modulation with corresponding maximum amplification and response amplitude being achieved by smaller hot temperature values. This implies that, for high frequencies, the maximum position of these quantities diminish and the dependence degenerate into monotonically decreasing function. In the contrary, the SNR displays no significant frequency dependence of position of its maximum values on the modulation frequencies.

5. The measures of the stochastic resonance phenomena such as spectral amplification and signal-to-noise-ratio observed in the course of numerical investigations for the high barrier limit approach shows very good qualitative agreement with the exact numerical technique.
6. The obtained results of our work admit to conclude that the phenomena of stochastic resonance effect is nicely visualized through the quantifiers studied.
7. The performed course of our numerical investigation has revealed important issues which appeal for further investigation. In particular, the model can be used to conduct an experiment to study the behavior of stochastic resonance provided that one is able to design a tunable laser beam's intensity so that the hot locality can easily be controlled which in turn controls the potential barrier.

Appendix

This program simulates the position of a Brownian particle in a two state model for a single realization and different noise strengths.

```
 $\Delta T = 0.5;$   
 $T_{max} = 1000;$   
 $N = T_{max}./\Delta T;$   
 $kappa = \text{input}(\text{'Enter the noise strength : '});$   
 $\text{store} = \text{zeros}(N, 2); \Delta V = 0.25; Amp = 0.1;$   
 $t = 0;$   
 $x_{old} = -1;$   
 $r_k = 1./(\pi * \sqrt{(2)}) . * \exp(-[\Delta V./kappa]);$   
 $Omega = \pi . * r_k$   
 $\text{for } i = 1 : N$   
 $t = t + \Delta T;$   
  
 $p_{net} = 2 . * r_k . * \Delta T . * \cosh(Amp . * x_{old} * \cos(Omega . * t));$   
  
 $r = \text{rand};$   
 $zi = r * \sqrt{(2 . * kappa * \Delta T)};$   
 $x_{new} = x_{old} - x_{old}.^3 . * \Delta T + x_{old} . * \Delta T + Amp . * \cos(Omega . * t) . * \Delta T + zi;$   
 $\text{store}(i,1:2) = [t \ x_{new}];$ 
```

```
if  $p_{net} \geq r$ 
     $x_{old} = -sign(x_{old});$ 
 $x_{new} = x_{old};$ 
else
 $x_{old} = x_{old};$ 
 $x_{new} = x_{old};$ 
endend

plot(store(:,1),store(:,2)); title('Single realization of x(t) in
the periodically modulated double well potential')
xlabel('time(sec)');
ylabel('x(t)');
```

Bibliography

- [1] Adi R. Bulsara and L. Gammaitoni, Phys Today, 39, March (1996).
- [2] L. Gammaitoni, P. Hanggi, P. Jung, F. Marchesoni, Rev. Mod. Phys. **70**, 223 (1998).
- [3] B. McNamara and K. Wiesenfeld, Phys. Rev. **A39**, 4854 (1989).
- [4] P. Hanggi, Chemphyschem, **3**, 285 (2002).
- [5] F. Guo, Y. R. Zhou, S. Q. Jiang and T. X. Gu, J. Phys. A: Math. Gen. **39**, 13861 (2006).
- [6] T. Wellens, V. Shatokhin and A. Buchleitner, Rep. Prog. phys. **67**, 45 (2004).
- [7] F. C. Bloudeau, *Lecture notes in physics*, **550** Springer (Berlin), 137 (2000).
- [8] Y. Jia, S. Yu and J. Li, Phys. Rev. E **62**, 1869 (2000).
- [9] N. G. van Kampen, IBM J. Res. Dev. **32**, 107 (1988).
- [10] Berhanu Aragie, M.Sc thesis, Addis Ababa University, Addis Ababa, July 2003 (unpublished).
- [11] N. G. van Kampen, Disorderd solids, structure and processes, edited by B. Di. Bartolo (Plenum Press, New York, 1989).

- [12] N. G. van Kampen J. Phys. Chem. Solids **49**, 673 (1988).
- [13] C. W. Gardiner, *Handbook of stochastic methods for Physics, Chemistry and Natural science* 2nd edition (Springerverlag, Berlin, 2003).
- [14] R. Benzi, Cond-mat/0702008.
- [15] P. V. E. McClintock, Nature, **443**, 635 (2006).
- [16] R. L. Badzey and P. Mohanty, Nature, **437**, 995 (2005).
- [17] R. Lofstedt and S. N. Coppersmith, Phys. Rev. E **49**, 4821 (1994).
- [18] M. V. Tretyakov, Phys. Rev. E **57**, 4789 (1998).
- [19] Y. G. Leng, T. Y. Wang, Y. Guo, Y. G. Xu, S. B. Fan, Science direct, **21**, 138 (2007).
- [20] S. S. Sastry, *Introductory methods of numerical analysis* 3rd edition (Prentice-Hall, New Delhi, 2003).
- [21] M. Bekele, V. Narayan and S. Stafstrom, (2005)(unpublished).
- [22] V. Narayan and M. Willander, Phys. Rev. B, **65**, 075308 (2002).
- [23] P. Riemann, Cond-mat/0010237.
- [24] R. Lahiri, Arvind and A. Sain, Cond-mat/0207246.
- [25] J. F. Beausang, arxiv: q - bio. BM/0610007
- [26] Arfken and Weber, *Mathematical methods for physicists fifth* edition (Academic press, USA, 2001)

DECLARATION

I hereby declare that this thesis is my original work and has not been presented for a degree in any other university. All sources of material used for the thesis have been duly acknowledged.

Name: *Bekele Jemama*
Signature:_____

This thesis has been submitted for examination with my approval as University advisor.

Name: *Dr. Mulugeta Bekele*
Signature:_____

Addis Ababa University
Department of Physics
July, 2007